

DIRECT SIMULATION OF LOW-DENSITY HYPERSONIC FLOW OVER A FORWARD-FACING STEP

Paulo H. M. Leite, phmineiro@lcp.inpe.br

Wilson F. N. Santos, wilson@lcp.inpe.br

National Institute for Space Research, Combustion and Propulsion Laboratory, Cachoeira Paulista-SP, 12630-000 BRAZIL

Abstract. *This work describes a computational investigation on rarefied hypersonic flow past forward-facing steps. Effects on the flowfield structure due to variations on the step height have been investigated by employing the Direct Simulation Monte Carlo (DSMC) method. The results presented highlight the sensitivity of the primary flow properties, velocity, density, pressure and temperature, to changes on the frontal-face height. It was found that the recirculation region ahead of the steps is a function of the frontal-face height. The analysis also showed that the extension of the upstream disturbance depends on the frontal-face height.*

Keywords: *DSMC, Hypersonic Flow, Rarefield Flow, Forward-Facing Step.*

1. INTRODUCTION

In the design of a hypersonic vehicle, the knowledge of the factors that affect the thermal and aerodynamic loads acting on the vehicle surface becomes imperative. Usually, in the calculations of the thermal and aerodynamic loads, the analysis assumes that the vehicle has a smooth surface. However, discontinuities, such as gaps, steps and cavities, are often present on the vehicle surface due to, for instance, fabrication tolerances, sensor installations, and differential expansion or ablation rates between non-similar materials (Bertram and Wiggs, 1963, Grotowsky and Ballmann, 2000, Hahn, 1969, and Nestler et al., 1969). Such surface discontinuities may constitute in a potential source in a heat flux rise to the surface or even though in a premature transition from laminar to turbulent flow.

In hypersonic flight, the flow over a step, gap or cavity causes locally thermal and aerodynamic loads which may dramatically exceed the ones of a smooth contour. In order to operate safely, these loads have to be predicted correctly. This can be done either by experiments which are often very expensive for real flight conditions or by numerical simulation, which is getting continuously increasing importance.

A large amount of gap, step and cavity research studies are available in the published literature. For the purpose of this introduction, it will be sufficient to describe only a few of these works. Nestler et al. (1969) conducted an experimental investigation on steps and cavities in a hypersonic turbulent flow. For the flow conditions investigated, they found that the pressure distributions in the cavity presented a typical behavior of closed cavity flow in the sense that the flow expands into the cavity, reattaches to the floor, and separates as it approaches the downstream corner.

Gai and Milthorpe (1995) presented experimental and computational results of a high-enthalpy flow over a blunted-stepped cone. Basically, an axisymmetric rearward-facing step of height of 0.15 and 0.3 times the nose radius of the cone. The analysis showed that the heat transfer rate is typical of that in separated flow, i.e., a sudden fall in heat transfer very near the step and then a gradual increase. The experimental data showed a decrease in heat transfer after reattachment, whereas the numerical prediction exhibited a plateau for a considerable distance.

Grotowsky and Ballmann (2000) investigated laminar hypersonic flow over forward- and backward-facing steps by employing Navier-Stokes equations. The hypersonic flow over the steps were simulated by considering freestream Mach number of 8, Reynolds number of the order of 10^8 and an altitude of 30 km. According to them, the computational results presented a good agreement with the experimental data available in the literature. They also pointed out that the quantitative comparison exhibited major differences for the wall heat flux, probably due to the difficulty in how to measure accurately.

According to the current literature, there have been considerable experimental and theoretical studies conducted to understand the physical aspects of hypersonic flow past to steps. The major interest in these studies has gone into considering laminar or turbulent flow in the continuum flow regime. However, there is little understanding of the physical aspects of hypersonic flow past to steps related to the severe aerothermodynamic environment associated to a reentry vehicle. In this scenario, the purpose of the present account is to investigate the flowfield structure of a hypersonic flow on a forward-facing step in the transition flow regime, i.e., between the continuum flow and the free collision flow regime. Therefore, the focus of the present study is the low-density region in the upper atmosphere, where numerical gaskinetic procedures are available to simulate hypersonic flows. High-speed flows under low-density conditions deviate from a perfect gas behavior because of the excitation of rotational and vibrational modes. At high altitudes, and therefore, low density, the molecular collision rate is low and the energy exchange occurs under non-equilibrium conditions. In such a circumstance, the degree of molecular non-equilibrium is such that the Navier-Stokes equations are inappropriate. Consequently, the Direct Simulation Monte Carlo (DSMC) method will be employed to calculate the hypersonic two-dimensional flow on a forward-facing step.

2. GEOMETRY DEFINITION

In the present account, the imperfections or distortions present on the surface of a reentry capsule is modeled by a forward-facing step. By considering that the step frontal-face h is much smaller than the nose radius R of a reentry capsule, i.e., $h/R \ll 1$, then, the hypersonic flow over the step may be considered as a hypersonic flow over a flat plate with a forward-facing step. Figure 1(a) displays a schematic view of the model employed and presents the important geometric parameters.

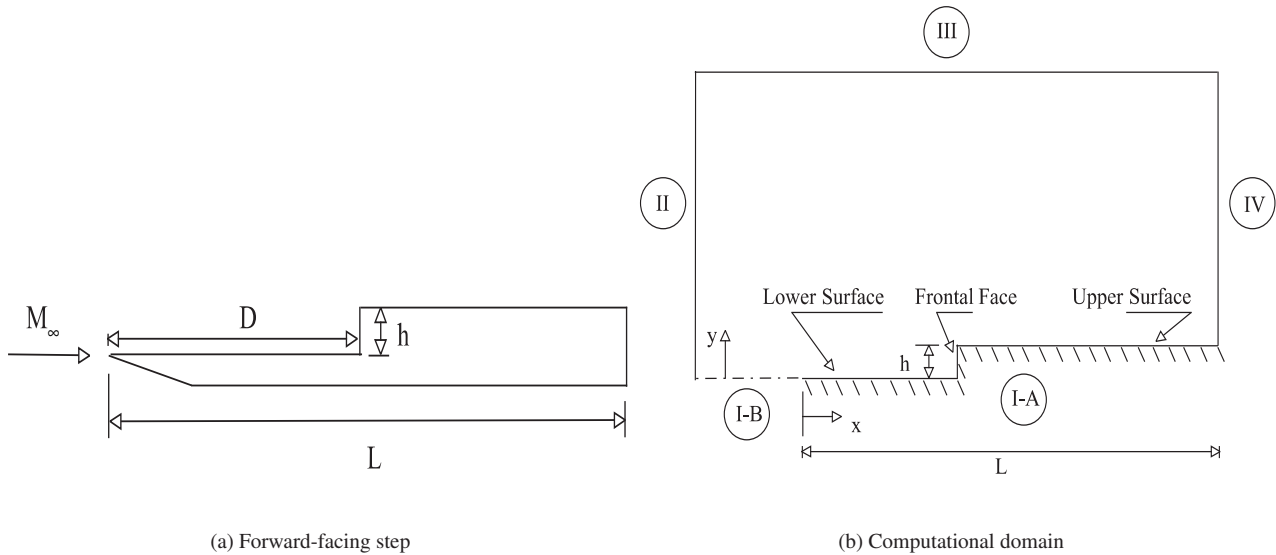


Figure 1. Drawing illustrating (a) the forward-facing step and (b) the computational domain.

According to Fig. 1(a), M_∞ represents the freestream Mach number, h the frontal-face height, L the total length of the forward-facing step, and D the location of the step. The distance D may be understood as being the distance from the stagnation point of the capsule to the step position on the capsule surface. It was considered that the forward-facing step is infinitely long but only the length L is considered. It was assumed frontal-face height h of 3, 6 and 9 mm, D/λ_∞ of 50 and D/λ_∞ of 100, where λ_∞ is the freestream mean free path.

An understanding of the frontal-face height impact on the flowfield structure can be gained by comparing the flowfield behavior of a flat plate with a step to that of a plate without a step. In this fashion, a flat plate free of imperfections, i.e., without steps works as a benchmark for the cases with steps.

3. COMPUTATIONAL METHOD AND PROCEDURE

The Direct Simulation Monte Carlo (DSMC) method (Bird, 1994) is a computational technique for modeling complex transitional flows of engineering interest. The DSMC method model a gas flow by using a computer to track the trajectory of simulated particles, where each simulated particle represents a fixed number of real gas particles. The direct simulation of the physical processes is in contrast with computation fluid dynamics (CFD) method that is applied to the mathematical equations that model the physical processes. The uncoupling of the molecular motion and collisions over small time steps and the division of the flowfield into small cells are the key computational assumptions associated with the DSMC method. The method has been tested in the transition flow regime in the last 40 years, and has shown excellent results when compared with experimental data (Harvey, 1986, 2000 and 2003, Holden and Wadhams, 2003).

Collisions in the present DSMC code are simulated with the variable hard sphere (VHS) molecular model (Bird, 1981) and the no time counter (NTC) collision sampling technique (Bird, 1989). Energy exchange between kinetic and internal modes is controlled by the Borgnakke-Larsen statistical model (Borgnakke and Larsen, 1975). For the present account, the simulations are performed using a non-reacting gas model, consisting of 76.3% of N_2 and 23.7% of O_2 , while considering energy exchange between translational, rotational and vibrational modes. For a given collision, the probability is defined by the inverse of the number of relaxation, which corresponds to the number of collisions needed, on average, for a molecule undergoes relaxation. The probability of an inelastic collision determines the rate at which energy is transferred between the translational and internal modes after an inelastic collision. Relaxation collision numbers of 5 and 50 were used for the calculations of rotation and vibration, respectively.

For the numerical treatment of the problem, the flowfield around the forward-facing step is divided into an arbitrary number of regions, which are subdivided into computational cells. The cells are further subdivided into subcells, two

subcells/cell in each coordinate direction. The cell provides a convenient reference for the sampling of the macroscopic gas properties, while the collision partners are selected from the same subcell for the establishment of the collision rate. The computational domain used for the calculation is made large enough so that body disturbances do not reach the upstream and side boundaries, where freestream conditions are specified. A schematic view of the computational domain is depicted in Fig. 1(b). According to this figure, side I-A is defined by the body surface. Diffuse reflection with complete thermal accommodation is the condition applied to this side. In a diffuse reflection, the molecules are reflected equally in all directions, and the final velocity of the molecules is randomly assigned according to a half-range Maxwellian distribution determined by the wall temperature. Side I-B is a plane of symmetry, where all flow gradients normal to the plane are zero. At the molecular level, this plane is equivalent to a specular reflecting boundary. Sides II and III are the freestream side through which simulated molecules enter and exit. Finally, the flow at the downstream outflow boundary, side IV, is predominantly supersonic and vacuum condition is specified (Bird, 1994). At this boundary, simulated molecules can only exit.

The numerical accuracy in DSMC method depends on the cell size chosen, on the time step as well as on the number of particles per computational cell. In the DSMC code, the linear dimensions of the cells should be small in comparison with the scale length of the macroscopic flow gradients normal to the streamwise directions, which means that the cell dimensions should be of the order of or smaller than the local mean free path (Alexander et al., 1998, Alexander et al., 2000). The time step should be chosen to be sufficiently small in comparison with the local mean collision time (Garcia and Wagner, 2000, and Hadjiconstantinou, 2000). In general, the total simulation time, discretized into time steps, is identified with the physical time of the real flow. Finally, the number of simulated particles has to be large enough to make statistical correlations between particles insignificant. These effects were investigated in order to determine the number of cells and the number of particles required to achieve grid independence solutions. Grid independence was tested by running the calculations with half and double the number of cells in the coordinate directions compared to a standard grid. Solutions (not shown) were near identical for all grids used and were considered fully grid independent.

4. FREESTREAM AND FLOW CONDITIONS

The flow conditions represent those experienced by a capsule at an altitude of 70 km. This altitude is associated with the transitional flow regime, which is characterized by the overall Knudsen number of the order of or larger than 10^{-2} . In this manner, the freestream conditions employed in the present calculations are those given by Bertin (1994) and listed in Tab. 1, and the gas properties (Bird, 1994) considered in the simulation are shown in Tab. 2.

Table 1. Freestream flow conditions

Altitude (km)	T_∞ (K)	p_∞ (N/m ²)	ρ_∞ (kg/m ³)	μ_∞ (Ns/m ²)	n_∞ (m ⁻³)	λ_∞ (m)
70	219.69	5.582	8.753×10^{-5}	1.455×10^{-5}	1.8192×10^{21}	9.285×10^{-4}

The freestream velocity U_∞ is assumed to be constant at 7456 m/s, which corresponds to a freestream Mach number M_∞ of 25. The wall temperature T_w is assumed constant at 880 K. This temperature is chosen to be representative of the surface temperature near the stagnation point of a reentry capsule and is assumed to be uniform over the forward-facing step. It is important to mention that the surface temperature is low compared to the stagnation temperature of the air. This assumption seems reasonable since practical surface material will probably be destroyed if surface temperature is allowed to approach the stagnation temperature.

By assuming the frontal-face height h as the characteristic length, the Knudsen number Kn_h corresponds to 0.3095, 0.1548 and 0.1032 for height h of 3, 6 and 9 mm, respectively. Finally, the Reynolds number Re_h , also based on the frontal-face height h and on conditions in the undisturbed stream, is around 136, 272, and 409 for height h of 3, 6 and 9 mm, respectively.

5. COMPUTATIONAL RESULTS AND DISCUSSION

The purpose of this section is to discuss and to compare differences in the flowfield properties due to variations on the frontal-face height of the forward-facing step. The flowfield properties of particular interest in this work are velocity, density, pressure and temperature.

Table 2. Gas properties

	X	m (kg)	d (m)	ω
O_2	0.237	5.312×10^{-26}	4.01×10^{-10}	0.77
N_2	0.763	4.650×10^{-26}	4.11×10^{-10}	0.74

5.1 Velocity Field

The DSMC method is essentially a statistical method. In this way, the macroscopic properties are computed as averages from the microscopic properties in each cell in the computational domain. As a result, the vector velocity is given by the following expression,

$$\mathbf{c}_0 = \frac{\sum_{j=1}^N (m\mathbf{c})_j}{\sum_{j=1}^N m_j} \tag{1}$$

where N , m and \mathbf{c} represent, respectively, the number of molecules, the mass and the velocity vector of the molecules in each cell. It should be noted that the mean molecular velocity $\bar{\mathbf{c}} (\equiv \mathbf{c}_0)$ defines the macroscopic mean velocity. It is important to mention that the velocity of the molecule relative to the mean macroscopic velocity, defined as thermal or peculiar velocity, is denoted by $\mathbf{c}' \equiv \mathbf{c} - \mathbf{c}_0$.

The distribution of tangential velocity u/U_∞ to three sections along the lower surface is illustrated in Fig. 2 as a function of the frontal-face height h . In this set of graphs, X represents the distance x normalized by the freestream mean free path λ_∞ , and Y the distance y above the lower surface also normalized by λ_∞ . As a basis of comparison, the velocity profile for the flat plate are illustrated in the same set of graphs.

Important features can be observed in the profiles of tangential velocity shown in Fig. 2. For sections $X \leq 30$, the velocity profiles for the step cases are identical by visual inspection with those for the flat-plate case. It means that no effect of the presence of the step is observed. However, for sections $X \geq 40$, the upstream disturbance caused by the step is observed on the velocity profiles. It is important to mention that the steps are placed at section $X = 50$. In addition, it is observed that the velocity profile is affected more upstream with increasing the step height h . This behavior results from the diffusion of molecules that are reflected from the frontal face of the step. As a result, by increasing the Reynolds number Re_h , the upstream disturbance increases, as would be expected. Also, for sections $X \geq 40$, the velocity profiles related to the steps indicate negative velocities near the lower surface, characterizing a recirculation region at the vicinity of the frontal face. This behavior in a rarefied flow, i.e., the presence of a recirculation region, also occurs in a continuum flow regime (Camussi et al., 2008).

Another peculiarity of the flow is with respect to the tangential velocity for $Y \approx 0$, i.e., the velocity along the flat-plate surface and along the lower surface of the step for sections far from the frontal face. It is clearly seen that $u/U_\infty \neq 0$ for $Y \approx 0$, a characteristic of a rarefied flow. As a result, the condition of $u/U_\infty = 0$ at the body surface, no-slip velocity in the continuum flow regime, is not applied in rarefied flow.

In order to emphasize important features in the flowfield structure, streamline traces at the vicinity of the steps are demonstrated in Fig. 4. In this group of diagrams, Y_h stands for the vertical distance y normalized by the step height h , and X'_h refers to the horizontal distance $x - D$ also normalized by the step height h . In this context, the reference frame was moved to the step position. According to Fig. 4, it is clearly noticed that, for the conditions investigated in the present account, it appears a recirculation region at the vicinity of the frontal face of the steps.

The following features are notable in Fig. 3. For the $h = 3$ mm case, the streamlines are parallel to the lower surface at the section $X'_h = -4.0$. Therefore, it is thus firmly established that the flowfield to $X'_h \leq -4.0$ has no idea about the

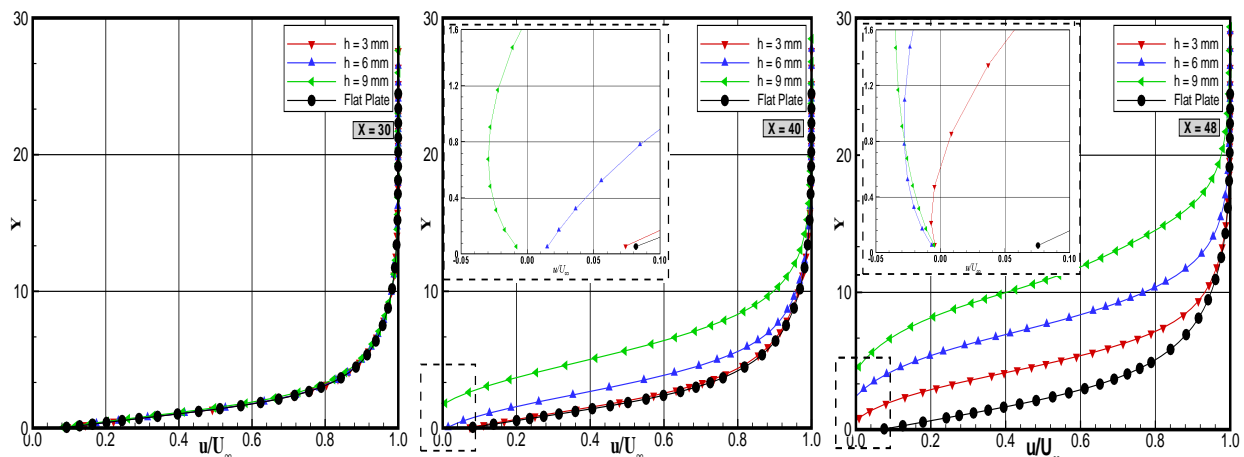


Figure 2. Distribution of tangential velocity (u/U_∞) along the lower surface of the forward-facing step as function of the height h .

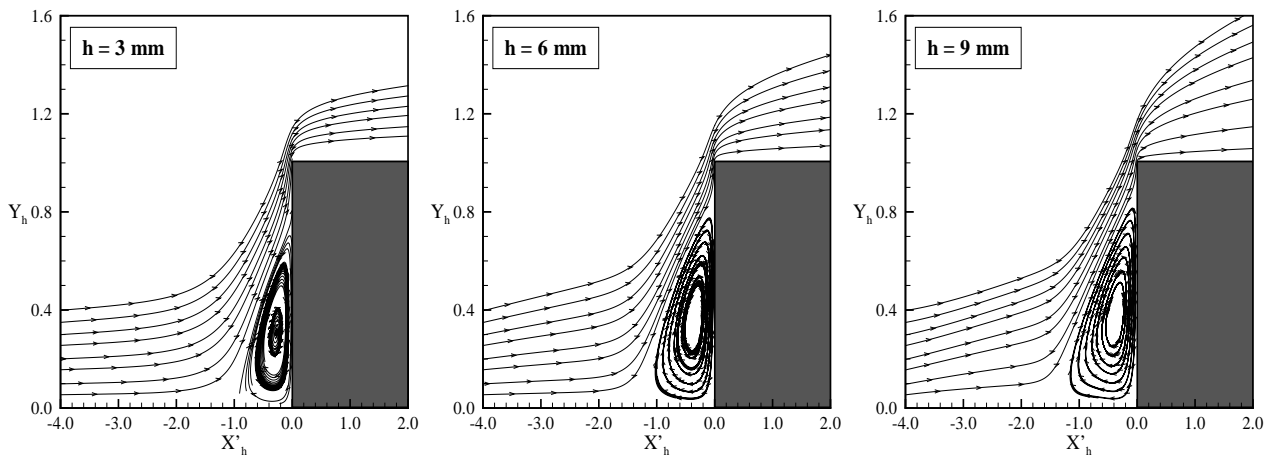


Figure 3. Distribution of streamline traces at the vicinity of the forward-facing step with height h of 3 mm (left), 6 mm (middle) e 9 mm (right).

presence of the step. In contrast, for the $h = 6$ and 9 mm cases, the streamlines are inclined upward at the same section, an indication that the flowfield knows about the presence of the step downstream along the lower surface. This information about the presence of the step is sent upstream through the collisions of the molecules.

Another flow peculiarity is related to the recirculation region. It may be inferred in passing that the recirculation region increases with increasing the step height h , or by increasing the Reynolds number Re_h , not only along the lower surface but also along the frontal face. This behavior differs from that one observed in a continuum flow regime. Based on an experimental investigation, Camussi et al.(2008) pointed out that the separation region occurs independently of the Reynolds number Re_h ; the separation region is of the order of a h upstream the step and approximately a half h size along the frontal face.

Still referring to Fig. 3, it is quite apparent that, after the flow separation on the lower surface, the flow reattaches at the vicinity of the shoulder of the step on the frontal face. For the steps under investigation, the point of separation x_s and the reattachment point y_r on the frontal face are obtained by assuming that $\tau_w = 0$, i.e., the section where the shear stress is equal to zero. The table 3 tabulates x_s and y_r as a function of the height of the step. In this table, X_s and X_{sh} represent the separation point x_s normalized by the freestream mean free path λ_∞ and by the step height h , respectively. Also, X'_{sh} correspond to $x_s - D$ normalized by the step height h . Similarly, Y_r and Y_{rh} stand for the point y_r normalized by λ_∞ and h , respectively.

Table 3. Separation and reattachment points of the flowfield as a function of the step height h .

h	X_s	X_{sh}	X'_{sh}	Y_r	Y_{rh}
3 mm	48.332	14.959	-0.516	2.635	0.815
6 mm	42.866	6.634	-1.104	5.619	0.869
9 mm	37.340	3.852	-1.306	8.707	0.898

5.2 Density field

The density in each cell in the computational domain is obtained by the following expression,

$$\rho = \frac{1}{V_c} \sum_{j=1}^N m_j \quad (2)$$

where N is the number of molecules in the cell, m is the mass of the molecules and V_c is the volume of the cell.

The distribution of density profiles ρ/ρ_∞ for three sections along the lower surface of the step is displayed in Fig. 4 as function of the step height h . Similar to the distribution of tangential velocity, the distribution of density profiles is shown in this set of plots to three sections defined by $X = 30, 40$ and 48 . Again X represents the distance x normalized by the freestream mean free path λ_∞ , and Y the distance y above the lower surface also normalized by λ_∞ . As a basis of comparison, density profiles for the flat-plate case are also presented in the same figure. Due to the large range of variation for the ratio ρ/ρ_∞ along the lower surface of the step, the scale in the x -direction differs from one plot to each other.

According to Fig. 4, it is seen that the upstream disturbance imposed by the step with h of 9 mm is felt by the density profile at section $X = 30$. In contrast, at section $X = 40$, there is no indication that the density profile be affected by the

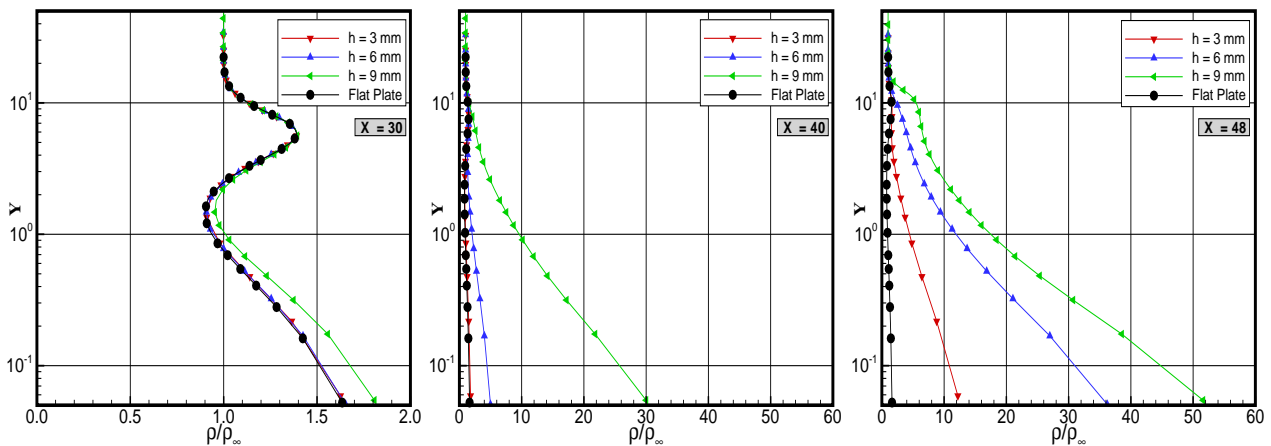


Figure 4. Distribution of density ratio (ρ/ρ_∞) profile along the lower surface of the forward-facing step as a function of the height h

presence of the step with $h = 3$ mm. As expected, by increasing the frontal face h , the disturbance caused by the step is felt more upstream in the flow. It should be mentioned in this context that, for $X < 30$, the density profiles for the step cases are identical to those presented for the flat-plate case.

Another flow peculiarity is observed in the Fig. 4. It is noted that density dramatically increases as the flow approaches the step, i.e., the density ρ increased by an order of magnitude when compared to the freestream density ρ_∞ . This density rise at the vicinity of the frontal face is a characteristic observed in blunt-body reentry flow, known as a cold-wall flow. Usually, in a reentry flow, the wall temperature T_w is low compared to the stagnation temperature T_o . For this particular investigation, this ratio is 0.032.

Still referring to Fig. 4, it is quite apparent that the density ratio shows significant changes in the direction perpendicular to the lower surface of the step. In the Y -direction, the density has a great value when compared to the freestream density. As Y increases from zero, density decreases very fast within a layer of the order of a molecular mean free path λ_∞ . In the following, by increasing Y , density increases further due to the shock wave, and finally decreases again reaching the value of the freestream density, for large values of Y . This behavior is usually observed when the temperature of the body surface is much lower than the stagnation temperature of the gas from the freestream. As a result, the gas near the wall tends to be very cold and denser than the rest of the gas in the boundary layer.

In a second stage of the investigation on the density behavior, it becomes instructive to explore the upstream disturbance in the flow, due to the presence of the step. A more careful examination was carried out in order to estimate the extent of this effect. For the first row of cells adjacent to the lower surface, the difference in the density was obtained for the two cases simulated, i.e., between the case with a step and the case and without step; the flat-plate case. In this scenario, $\Delta\rho_x$ denotes the density rise, due to the presence of the step, as a function of the x coordinate. Figure 5(a) illustrates the extent of this effect along the lower surface. In this figure, the density difference $\Delta\rho_x$ is normalized by the freestream density ρ_∞ . Also, X'_h refers to the horizontal distance $x - D$ normalized by the frontal-face height h .

Looking first to Fig. 5(a), it is observed that the presence of the step causes a significant increase in density at the vicinity of the step. It is seen that $\Delta\rho_x/\rho_\infty$ has a continuous increase up to the frontal face for the $h = 3$ mm case. Nevertheless, for the other two cases, h of 6 e 9 mm, $\Delta\rho_x/\rho_\infty$ exhibits a plateau, well defined for the $h = 9$ mm case. By considering the position in which the plateau takes place, there is an indication that it is related to the recirculation region.

Still referring to Fig. 5(a), it is clearly noticed that the region affected by the presence of the step is a function of the step height h . By considering $\Delta\rho_x/\rho_\infty = 0.05$ as the limit condition, then this condition is associated to a position denoted by the interaction point x_0 . Hence, based on the reference system shown in Fig. 5(a), the interaction point X'_{0h} is approximately -3.68, -2.74 and -2.26 for h of 3, 6 e 9 mm, respectively. For comparison purpose, if normalized by the freestream mean free path λ_∞ , the interaction point X'_0 corresponds to 38.12, 32.27 and 28.05, for h of 3, 6 and 9 mm, respectively. The difference between the point of separation x_s , and the point of interaction x_0 , determines the pre-separation region, defined here by x_{ps} . The pre-separation region defines the distance before the separation that a particular macroscopic property indicates to be affected by the presence of the step in the flow. The Table 4 summarizes the interaction point and the pre-separation region for density. For convenience, the values for the interaction point and the pre-separation region for pressure (inside parenthesis) and for translational temperature (inside brackets) are also tabulated in Tab. 4. Nevertheless, these properties will be discussed subsequently. In this table, X_0 and X_{ps} stand for the interaction point and the pre-separation region normalized by the freestream mean free path λ_∞ , respectively. In a similar way, X'_{0h}

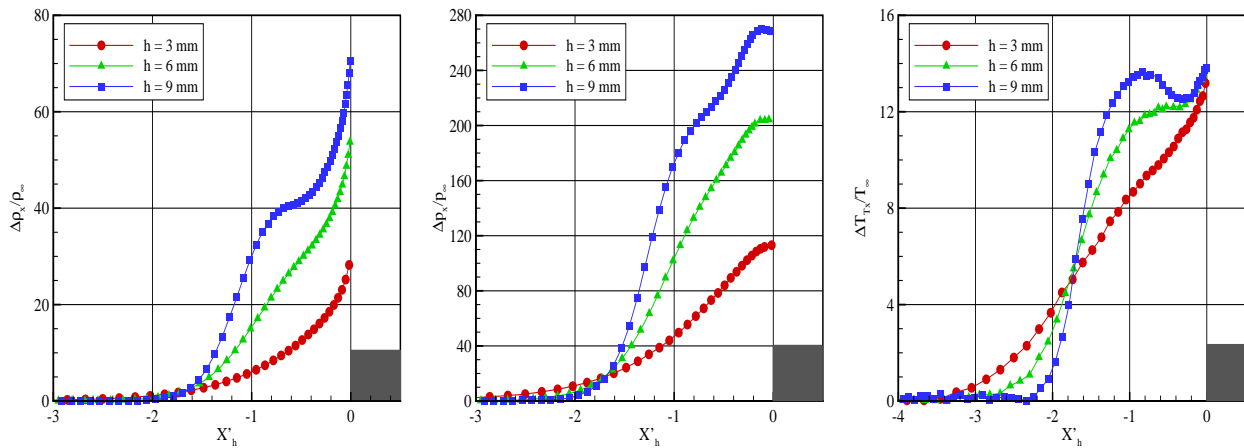


Figure 5. Upstream disturbance effect on density (left side), on pressure (middle) and on translational temperature (right side) due to the presence of the forward-facing step.

Table 4. Point of interaction and the pre-separation region related to the density, (pressure), and [translational temperature] as a function of the height h .

h	X_0	X_{ps}	X'_{0h}	X'_{ps}
3 mm	38.12 (37.83) [38.41]	10.21 (10.50) [9.92]	-3.68 (-3.77) [-3.59]	3.16 (3.25) [3.07]
6 mm	32.27 (33.79) [28.42]	10.69 (9.08) [14.45]	-2.74 (-2.51) [-3.34]	1.64 (1.41) [2.24]
9 mm	28.05 (28.20) [27.59]	9.29 (9.14) [9.75]	-2.26 (-2.25) [-2.31]	0.95 (0.94) [1.01]

and X'_{ps} represent the interaction point and the pre-separation based on the reference system located at the step position, normalized by the height h .

5.3 Pressure field

The pressure in each cell inside de computational domain is obtained by the following equation,

$$p = \frac{1}{3V_c} \sum_{j=1}^N \frac{(mc'^2)_j}{N} \quad (3)$$

where N is the number of molecules in the cell, m is the mass of the molecules and V_c is the volume of the cell and c' is the thermal velocity of the molecules.

The distribution of pressure profiles p/p_∞ for three sections along the lower surface of the step is illustrated in Fig. 6 as function of the step height h . In this set of plots, the pressure profiles are shown to three sections defined by $X = 30, 40$ and 48 . It is important to emphasize that, due to the large range of variation for the ratio p/p_∞ along the lower surface of the step, the scale in the x -direction differs from one plot to each other.

According to Fig. 6, it is seen that the pressure profiles follow the same behavior as those presented by the density profiles. The pressure profile for the step cases are identical to those obtained for the flat-plate case up to section $X = 30$. For sections defined by $X > 30$, the pressure field is affected by the presence of the steps. It is somewhat surprising to find that, at the vicinity of the frontal face, the pressure p dramatically increased two orders of magnitude as compared to the freestream pressure p_∞ .

The upstream disturbance in the pressure field, due to the presence of the steps, was estimated in a similar way as that presented by density. In this fashion, for the first row of cells along the lower surface, the difference in pressure Δp_x was calculated for the two investigations, i.e., pressure for the flat-plate case with steps minus pressure for the flat-plate case without steps. As calculated along the lower surface, the Δp_x represents the pressure rise due to the presence of the steps.

Figure 5(b) displays the extent of this effect along the lower surface. In this figure, the pressure difference Δp_x is normalized by the freestream pressure p_∞ . Based on Fig. 5(b), it is noted that the region affect by the presence of the steps is a function of the frontal-face height. Also, it is very encouraging to observe that the the pressure difference

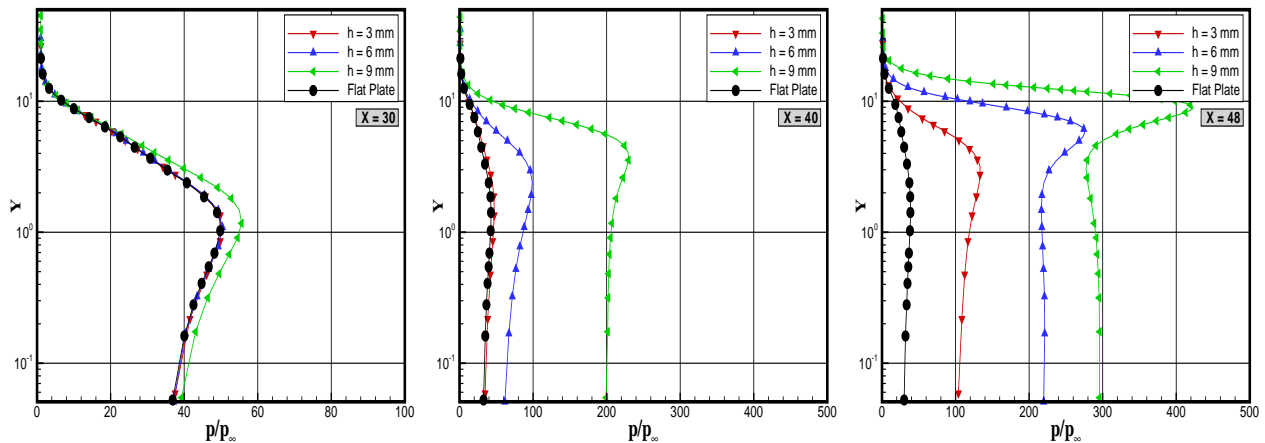


Figure 6. Distribution of density ratio (p/p_∞) profile along the lower surface of the forward-facing step as a function of the height h

$\Delta p_x/p_\infty$ exhibits a plateau at the vicinity of the frontal face. It should be remarked that, the presence of plateau in the pressure was also observed by Chapmann et al. (1958) that conducted an experimental investigation on steps in the continuum flow regime.

By the time being, it proves convenient to define the interaction point and the pre-separation region related to the pressure field. Similarly to the density field, these properties were also estimated and are tabulated in Tab. 4. In this table, the data related to pressure are listed inside the parenthesis. As indeed is clear from the Tab. 4, the interaction point and the pre-separation region for pressure are very close to those for density.

5.4 Kinetic temperature field

The strong shock wave that forms around the forward-face step at hypersonic flow converts part of the kinetic energy of the freestream air molecules into thermal energy. This thermal energy downstream of the shock wave is partitioned into increasing the translational kinetic energy of the air molecules, and into exciting other molecular energy states such as rotation and vibration.

Temperature ratio profiles along the lower surface are displayed in Fig. 7 for sections X of 30, 40 and 48. In this set of diagrams, temperature ratio stands for the translational temperature T_T , rotational temperature T_R , vibrational temperature T_V or overall temperature T_{OV} normalized by the freestream temperature T_∞ . Also, filled and empty symbols correspond to temperature distributions frontal-face height h of 3 and 9 mm, respectively. It is apparent from these diagrams that thermodynamic non-equilibrium occurs throughout the shock layer, as shown by the lack of equilibrium of the translational and internal kinetic temperatures. Thermal non-equilibrium occurs when the temperatures associated with translational, rotational, and vibrational modes of a polyatomic gas are different. In such a context, it proves convenient to define the overall kinetic temperature. The overall kinetic temperature shown is defined for a non-equilibrium gas as the weighted mean of the translational and internal temperature (Bird, 1994) as follows,

$$T_{OV} = \frac{3T_T + \zeta_R T_R + \zeta_V T_V}{3 + \zeta_R + \zeta_V} \quad (4)$$

where ζ is the degree of freedom and subscript T , R and V stand for translation, rotation and vibration, respectively.

The overall kinetic temperature T_{OV} is equivalent to the thermodynamic temperature only in thermal equilibrium conditions. As a matter of fact, it should be noticed that the ideal gas equation of state does not apply to this temperature in a non-equilibrium situation.

Still referring to Fig. 7, it is clearly seen that the frontal-face impact is more significant in the temperature profiles for sections at the vicinity of the step, i.e., for sections $X > 30$. Conversely, no appreciable changes are observed for sections $X < 30$. Of particular interest in the analysis is also the behavior of the overall kinetic temperature in comparison to the wall temperature T_w . According to the prescribed conditions, the wall temperature was set around four times the freestream temperature, i.e., $T_w/T_\infty = 4$. Therefore, the ratio of the overall kinetic temperature to the wall temperature, T_{OV}/T_w , is given by $0.25(T_{OV}/T_\infty)$. As a result, with this in mind, it is observed from Fig. 7 that the overall kinetic temperature reaches a value on the lower surface that is above the wall temperature, resulting in a temperature jump as defined in continuum formulation. It is clearly noticed that the downstream evolution of the flow along the lower surface

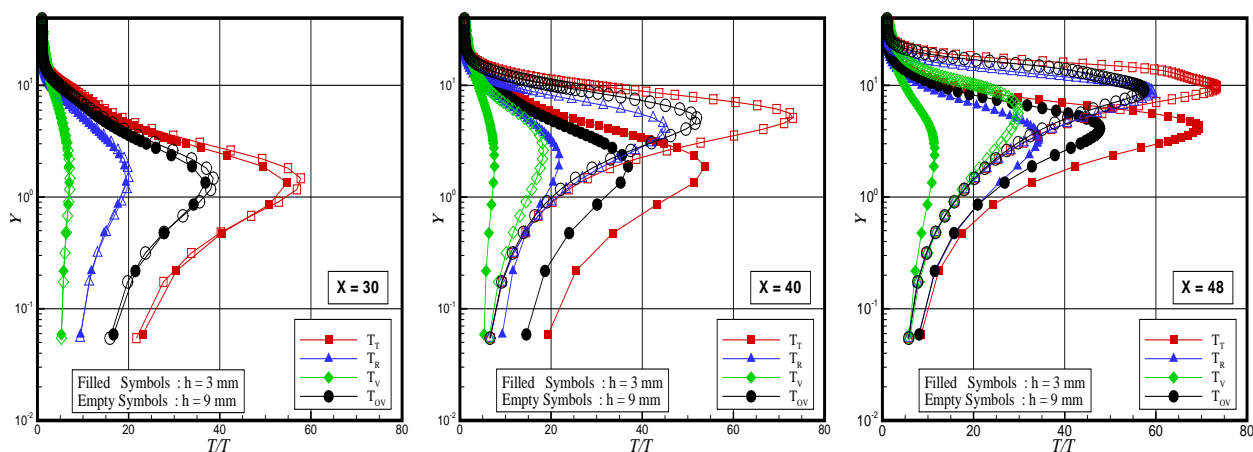


Figure 7. Distribution of kinetic temperature ratio (T/T_∞) profile along the lower surface of the forward-facing step as a function of the height h

displays a smearing tendency of the shock wave due to the displacement of the maximum value for the translational temperature as well as for the overall kinetic temperature. Also, it may be recognized from the overall kinetic temperature distribution that significant changes in the overall kinetic temperature profiles occur within a layer larger than $10\lambda_\infty$ for sections close to the frontal face.

For completeness, the computations discussed above on interaction point and pre-separation region for density and pressure were also performed by the translational temperature. Figure 5(c) exhibits the upstream disturbance in the temperature field. In this figure, the temperature difference ΔT_x is normalized by the freestream temperature T_∞ . Based on Fig. 5(c), it is observed that the region affect by the presence of the steps is a function of the frontal-face height, as would be expected. Finally, Tab. 4 tabulates the values (inside brackets) for interaction point and the pre-separation region associated to temperature. According to Tab. 4, the interaction point and the pre-separation region for temperature are very close to those for density and pressure. This is in contrast to the upstream disturbance observed in an hypersonic flow over a blunt body in the sense that the extent of the disturbance is significantly different for each one of the primary properties. The domain of influence for temperature is usually larger than that observed for pressure, density and velocity.

6. CONCLUDING REMARKS

Computations of a rarefied hypersonic flow on forward-facing steps have been performed by using the Direct Simulation Monte Carlo method. The calculations provided information concerning the nature of the flowfield structure about the primary flow properties at the vicinity of the steps. Effects of the frontal-face height on the velocity, density, pressure, and temperature for a representative range of parameters were investigated. The frontal-face height ranged from 3 to 9 mm, which corresponded Knudsen numbers in the transition flow regime.

It was found that the interaction point location and the separation region size upstream the steps are a function of the frontal-face height. The analysis showed that the upstream disturbance due to the presence of the steps increased with increasing the frontal-face height. In addition, the extent of this disturbance observed on the temperature field is similar to that on the pressure field and density field.

7. ACKNOWLEDGEMENTS

The authors would like to thank the financial support provided by CNPq (Conselho Nacional de Desenvolvimento Científico e Tecnológico) under Grant No. 473267/2008-0.

8. REFERENCES

- Alexander, F. J., Garcia, A. L., and, Alder, B. J., 1998, "Cell Size Dependence of Transport Coefficient in Stochastic Particle Algorithms", *Physics of Fluids*, Vol. 10, No. 6, pp. 1540–1542.
- Alexander, F. J., Garcia, A. L., and, Alder, B. J., 2000, "Erratum: Cell Size Dependence of Transport Coefficient is Stochastic Particle Algorithms", *Physics of Fluids*, Vol. 12, No. 3, pp. 731–731.
- Bertin, J. J., 1994, "Hypersonic Aerothermodynamics", AIAA Education Series, Washington DC.
- Bertram, M. H., and Wiggs, M. M., 1963, "Effect of Surface Distortions on the Heat Transfer to a Wing at Hypersonic

- Speeds”, *AIAA Journal*, Vol. 1, No. 6, pp. 1313–1319.
- Bird, G. A., 1981, “Monte Carlo Simulation in an Engineering Context”, *Progress in Astronautics and Aeronautics: Rarefied gas Dynamics*, Ed. Sam S. Fisher, Vol. 74, part I, AIAA New York, pp. 239–255.
- Bird, G. A., 1989, “Perception of Numerical Method in Rarefied Gasdynamics”, *Rarefied gas Dynamics: Theoretical and Computational Techniques*, Eds. E. P. Muntz, and D. P. Weaver and D. H. Capbell, Vol. 118, *Progress in Astronautics and Aeronautics*, AIAA, New York, pp. 374–395.
- Bird, G. A., 1994, “Molecular Gas Dynamics and the Direct Simulation of Gas Flows”, Oxford University Press, Oxford, England, UK.
- Borgnakke, C. and Larsen, P. S., 1975, “Statistical Collision Model for Monte Carlo Simulation of Polyatomic Gas Mixture”, *Journal of Computational Physics*, Vol. 18, No. 4, pp. 405–420.
- Camussi, R., Felli, M., Pereira, F., Aloisio, G., and Di Marco, A., 2008, “Statistical Properties of Wall Pressure Fluctuations over a Forward-Facing Step”, *Physics of Fluids*, Vol. 20, pp. 075113.
- Chapmann, D. R., Kuehn, D. M. and Larson, H. K., 1958, “Investigation of Separated Flows in Supersonic and Subsonic Streams with Emphasis on the Effect of Transition”, *NACA Report 1356*.
- Gai, S.L., and Milthorpe, J. F., 1995, “Hypersonic High-Enthalpy Flow over a Blunt-Stepped Cone”, *Proceedings of the 20th International Symposium on Shock Waves*, pp. 234–244.
- Garcia, A. L., and Wagner, W., 2000, “Time Step Truncation Error in Direct Simulation Monte Carlo”, *Physics of Fluids*, Vol. 12, No. 10, pp. 2621–2633.
- Grotowsky, M. G., and Ballmann J., 2000, “Numerical Investigation of Hypersonic Step-Flows”, *Shock Waves*, Vol. 10, pp. 57–72.
- Hadjiconstantinou, N. G., 2000, “Analysis of Discretization in the Direct Simulation Monte Carlo”, *Physics of Fluids*, Vol. 12, No. 10, pp. 2634–2638
- Hahn M., 1969, “Experimental Investigation of Separated Flow over a Cavity at Hypersonic Speed”, *AIAA Journal*, Vol. 7, No. 6, pp. 1092–1098.
- Harvey, J. K., 1986, “Direct Simulation Monte Carlo Method and Comparison with Experiment”, *Rarefied Gas Dynamics: Thermophysical Aspect of Re-entry Flows*, Eds. J. N. Moss and C. D. Scott, vol. 103, pp. 25–43, *Progress in Astronautics and Aeronautics*, AIAA, Washington, DC.
- Harvey, J. K., 2000, “Review of Code Validation Studies in High-Speed Low-Density Flows”, *Journal of Spacecraft and Rockets*, Vol. 37, No. 1, pp. 8–20.
- Harvey, J. K., 2003, “A review of a validation exercise on the use of the DSMC method to compute viscous/inviscid interactions in hypersonic flow”, *AIAA Paper 2003–3643*.
- Holden, M. S. and Wadhams, T. P., 2003, “A review of experimental studies for DSMC and Navier-Stokes code validation in laminar regions of shock/shock and shock/boundary layer interaction including real gas effects in hypersonic flows”, *AIAA Paper 2003–3641*.

9. Responsibility notice

The authors are the only responsible for the printed material included in this paper.